energies

MDPI

Article

Peukert Generalized Equations Applicability with Due Consideration of Internal Resistance of Automotive-Grade Lithium-Ion Batteries for Their Capacity Evaluation

Nataliya N. Yazvinskaya [1], Mikhail S. Lipkin [2], Nikolay E. Galushkin [3,*] and Dmitriy N. Galushkin [3]

[1] Department of Cybersecurity of Information Systems, Don State Technical University, 344000 Rostov-on-Don, Russia; lionnat@mail.ru
[2] Department of Chemical Technologies, Platov South-Russian State Polytechnic University, 346428 Novocherkassk, Russia; lip-kin@yandex.ru
[3] Laboratory of Electrochemical and Hydrogen Energy, Don State Technical University, 346500 Shakhty, Russia; dmitrigall@yandex.ru
* Correspondence: galushkinne@mail.ru; Tel.: +7-92-8769-7820

Abstract: In this paper, the applicability of the Peukert equation and its generalizations were investigated for capacity evaluation of automotive-grade lithium-ion batteries. It is proved that the classical Peukert equation is applicable within the range of the discharge currents from $0.2C_n$ to $2C_n$ (C_n is the nominal battery capacity). As a rule, the operating currents of many automotive-grade lithium-ion batteries are exactly within this range of the discharge currents. That is why, successfully, the classical Peukert equation is used in many analytical models developed for these batteries. The generalized Peukert equation $C = C_m/(1 + (i/i0)^n)$ is applicable within the discharge currents range from zero to approximately $10C_n$. All kinds of operating discharge currents (including both very small ones and powerful short-term bursts) fall into this discharge currents range. The modified Peukert equation $C = C_m(1 - i/i1)/((1 - i/i1) + (i/i0)^n)$ is applicable at any discharge currents. This equation takes into account the battery's internal resistance and has the smallest error of experimental data approximation. That is why the discussed modified Peukert equation is most preferable for use in analytical models of automotive-grade lithium-ion batteries. The paper shows that all the parameters of the generalized Peukert equations have a clear electrochemical meaning in contrast to the classical Peukert equation, where all the parameters are just empirical constants.

Keywords: Peukert equation; lithium-ion battery; capacity; automotive-grade battery; internal resistance

Citation: Yazvinskaya, N.N.; Lipkin, M.S.; Galushkin, N.E.; Galushkin, D.N. Peukert Generalized Equations Applicability with Due Consideration of Internal Resistance of Automotive-Grade Lithium-Ion Batteries for Their Capacity Evaluation. *Energies* **2022**, *15*, 2825. https://doi.org/10.3390/en15082825

Academic Editor: Carlos Miguel Costa

Received: 14 March 2022
Accepted: 12 April 2022
Published: 13 April 2022

1. Introduction

Currently, lithium-ion batteries are increasingly becoming widespread among both small-format batteries [1,2] and large-format batteries [2–5]. For optimal lithium-ion battery operation, both at the design stage and at the stage of their operation, reliable models of these batteries are needed. The most functional models of the batteries are based on the fundamental laws of physics and electrochemistry [6–8].

However, these models are not applicable in aviation and for electric vehicles [9]. First of all, those models are too complex and cannot be solved by onboard computers of electric vehicles or airplanes. In addition, fundamental electrochemical models require new and complex calibration when batteries of certain manufacturers or types are replaced with others. Many parameters of these models cannot be measured experimentally. For example, this concerns the parameters of the medium inside of the porous electrode. Usually, those parameters are found by fitting the model to the results of various experiments.

Therefore, in practice, the most often used are the battery analytical models [9–14] built up based on various empirical equations or the non-linear structural model [15]. In addition,

analytical models are used as part of complex fundamental electrochemical models when simulated processes are poorly understood (for example, the battery thermal runaway process [16–19], the process of the hydrogen accumulation in battery electrodes [20,21], Li–S batteries [22,23], etc.).

When using the batteries in electric vehicles, one first needs to know the battery's state of charge (SoC) as the electric vehicle's operation duration depends on this parameter. Currently, there are many ways to evaluate SoC. For example, the following methods are used to evaluate SoC: The open-circuit voltage measurement [24] can be used (however, in dynamic operation mode, this method gives an error up to 20% [25]). Additionally, models based on the Kalman filter are applicable [26–30] (with an error of up to 10% [31]). The most widely used method of SoC estimation is based on two parameters: the voltage profile and the ampere-hours counting consumed by the battery (however, this method contains a number of disadvantages, too [1]).

According to our experimental studies, the most reliable method of SoC finding is the assessment based on the Hausmann model [9]. The analytical Hausmann model calculating the battery's residual capacity is as follows:

$$C_t = C_m - \sum_{i=0}^{t} I_{eff}(i_i, T_i)\Delta t,\ I_{eff}(i_t, T_t) = f_1(i_t)f_2(T_t) = \gamma(i_t)^{\alpha}\left(\frac{T_{ref}}{T_t}\right)^{\beta}, \quad (1)$$

where Δt is the time-step; i_t, T_t, C_t are the current, temperature, and remaining capacity of the battery at time t; α, β, γ are empirical constants; C_m is the battery top capacity; T_{ref} is the reference temperature for the tested battery (298 K).

The Hausmann model (1) was developed specifically for the dynamic operation mode of electric vehicles. It works as follows: The entire range of the electric vehicle's operating time is divided into a series of very small time intervals (usually Δt = 1 s). In this case, the total released capacity of the battery will be equal to the sum of the released capacities at every time interval Δt. Within a very small time interval Δt, the current and temperature can be considered constant; therefore, within the time interval Δt, it is possible to use both the Peukert equation and the empirical equation describing the dependence of the battery capacity on the temperature.

It should be noted that the functions $I_{eff}(i,T)$ and $C(i,T)$ are related by the ratio [10]

$$C(i,t) = \frac{C_m}{I_{eff}(i,T)/i}. \quad (2)$$

Hence, within every time interval Δt (in the Hausmann model (1)), the released capacity is related to the discharge current and the battery temperature by the equation

$$C(i,T) = \frac{A}{i^n}\left(\frac{T}{T_{ref}}\right)^{\beta},\ n = \alpha - 1,\ A = C_m/\gamma. \quad (3)$$

Thus, in model (1), the Peukert equation (in Equation (3), this is the first multiplier) determines the dependence of the battery capacity on the discharge current $C(i)$. In contrast, the second multiplier $C(T)$ (3) determines the dependence of the capacity on the temperature of the battery.

In paper [10], it was experimentally proved that the function $C(T)$ has a much more sophisticated form over the entire range of battery temperature changes.

$$C(T) = K\frac{\left(\frac{T-T_k}{T_{ref}-T_k}\right)^{\beta}}{(K-1) + \left(\frac{T-T_k}{T_{ref}-T_k}\right)^{\beta}} \quad (4)$$

Indeed, $C(T)$ must be zero at the freezing point of the electrolyte (T_k) (4). However, in Equation (3), it turns out that $C(i,T) = 0$ at $T = 0$, which is wrong. K is an empirical constant.

Additionally, the equation from Peukert's paper [32] (which is written often as follows [9,10])

$$C = \frac{A}{i^n} \tag{5}$$

incorrectly describes the experimental equation $C(i)$ for lithium-ion batteries (Figure 1) both at low and high discharge currents. Indeed, when the discharge current decreases, the battery capacity in Peukert's Equation (5) tends to infinity, which has no physical meaning. At high discharge currents, the experimental function $C(i)$ is as shown in Figure 1.

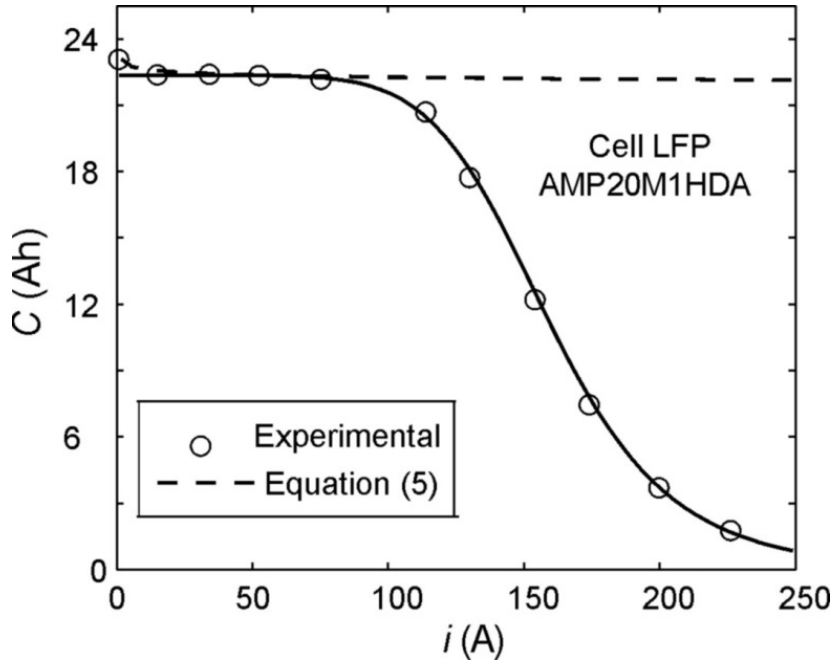

Figure 1. Comparison between experimental data for lithium-ion batteries and Peukert Equation (5).

It is fundamentally important that the experimental function $C(i)$ for the lithium-ion batteries has three absolutely different sections (Figure 1). The first section of function $C(i)$ is located at the currents from zero to the first curve inflection point (approximately 50 A). In this section, function $C(i)$ is concave. The second section of function $C(i)$ is located at the currents from the first inflection point to the second inflection point (approximately 150 A). In this section, function $C(i)$ is convex. The third section of function $C(i)$ covers the currents from the second inflection point to the maximum current values used. In this section, function $C(i)$ is concave again (Figure 1).

The Peukert Equation (5) describes only concave sections of function $C(i)$ (at $n > 0$) as the equation was obtained originally for lead-acid batteries whose capacity dependence on the discharge current is always concave.

However, the Peukert Equation (5) is used successfully in many models of lithium-ion batteries [9,10,33,34].

In our previous paper [31], it was proved that the operating currents of most parts of the small-format lithium-ion batteries fall within the discharge currents range of the first section of function $C(i)$ (where it is concave) (Figure 1). Therefore, the Peukert Equation (5) can be used in many models of lithium-ion batteries.

In paper [13], the generalized Peukert equation was obtained, which corresponds to the experimental values of function $C(i)$ at any discharge current for small-format lithium-ion batteries. It looks like the following:

$$C(i) = \frac{C_m}{1 + \left(\frac{i}{i0}\right)^n} \quad (6)$$

where C_m is battery top capacity, $C(i0) = C_m/2$.

However, at very high discharge currents, there is such a current as $i1$, at which, at the moment of the battery discharge mode turning on, the voltage at the battery terminals will be equal to the lower cutoff of voltage. Therefore, at current $i1$, when the battery discharge is turned on, the battery capacity will be zero. This fact is not taken into account by Equations (5) and (6). In paper [12], on the basis of the transformation of the Shepherd equation [35], it was proved that the internal resistance of the batteries is the reason for the existence of the extremely large discharge current $i1$. It should be noted that in Equations (5) and (6), the internal resistance of the batteries is not taken into account. If the internal resistance of the batteries is taken into consideration, the generalized Peukert Equation (6) for small-format lithium-ion batteries will take the following form [12]:

$$C(i) = \frac{C_m(1 - i/i1)}{(1 - i/i1) + \left(\frac{i}{i0}\right)^n} \quad (7)$$

$$i0 = \sqrt[n]{\frac{E - u_k - u_r}{K1}},\ i1 = \frac{E - u_k - u_r}{R} \quad (8)$$

where $i1$ is the current, at which $C(i1) = 0$; E is the electromotive force (EMF) of a fully charged battery; R is the internal resistance of the battery; u_r is the voltage drop due to the relaxation processes in the discharge process beginning; u_k is lower cutoff voltage.

This paper is aimed at the improvement of the Hausmann model (1) for the assessment of the residual capacity of the automotive-grade lithium-ion batteries using a more accurate, modified Peukert Equation (7).

2. Experiments, Methods, and Errors Calculation

In our experiments, we used commercial automotive-grade lithium-ion batteries of the types shown in Table 1.

Table 1. Characteristics of investigated commercial automotive-grade lithium-ion batteries.

Model	SE100AHA	LFP90	38120S	SLPB96255255
Manufacturer	CALB	ThunderSky	Headway	Kokam
Cathode material	$LiFePO_4$	$LiFePO_4$	$LiFePO_4$	$LiCoO_2$
Structure	prismatic battery	prismatic battery	cylindrical battery package (1S10P)	pouch battery
Nominal capacity (Ah)	100	90	100	60
Charge current (A)	40	40	40	30
Upper cutoff (V)	3.60	4.25	3.65	4.20
End-current (A)	2.5	2.25	2.5	1.5
Discharge current (for initial cycles) (A)	20	18	20	12
Lower cutoff (V)	2.50	2.50	2.00	2.70

The batteries were charged in the mode of constant current and constant voltage (CC/CV) in accordance with the parameters shown in Table 1. The discharge of the batteries was carried out in the constant current mode (CC) in accordance with the parameters shown in Table 1 (for initial cycles).

For battery charging, the electrochemical workstation ZENNIUM together with the potentiostat PP242 were used. The top operating current of the latter was ±40 A. The discharge process was performed with the electronic load ITECH IT8945-150-2500 (with

a top operating current of 2500 A). The battery temperature was measured with four temperature sensors attached to the battery on its sides in different places.

In order to stabilize the battery temperature during its discharge, the battery was placed into the climatic chamber Binder MK240 at a temperature of 25 °C. In addition, radiators (used for computer processors cooling down) were attached to the battery from all sides by a heat-conducting paste and special clamps. The radiators enhanced the heat exchange and the battery cooling down. As a result of those measures, the temperature of the batteries did not exceed 55 °C at any discharge currents.

Three batteries of each type were used in the experiments (Table 1).

The experimental research procedure consisted of the following stages:

Firstly, in order to stabilize the SEI layer of new batteries, eight initial cycles were performed in accordance with the parameters specified in Table 1. Nevertheless, if in the last three cycles, the resulting capacity differed by more than 5%, then an additional 3–5 initial cycles were performed (Table 1). If the stabilization capacity was still not possible, some batteries were replaced with new ones of the same type, and the experiment was started over again.

Secondly, the charge of the studied batteries was carried out in accordance with the parameters specified in Table 1. In the subsequent research-related cycles, the battery discharging was carried out at constant currents in a range from $0.2C_n$ up to around $10C_n$ (C_n is the nominal battery capacity).

Thirdly, at each discharge current, measurements were carried out for all three selected batteries of the same type. However, if the resulting capacity differed by more than 5%, some additional initial cycles were performed with the purpose of stabilizing the batteries up to 5%. If stabilization was not possible, some batteries were replaced with new ones of the same type, and the experiment started over again.

Fourthly, as an experimental value of the capacity at a certain discharge current, the value was taken, which was the average value of three measurements for three batteries of the same type.

Fifthly, before each measurement, three of the initial cycles were carried out (Table 1). These initial cycles needed to be carried out for two reasons. Firstly, in order to exclude the mutual influence of some discharge cycles on other discharge cycles. However, if the resulting capacity differed by more than 5% in the three initial cycles, some additional initial cycles were performed. If stabilization was not possible, some batteries were replaced with new ones of the same type, and the experiment started again in order to eliminate the effect of the loss of battery capacity due to their aging during cycling. Therefore, the average capacity of each battery in these three initial cycles was compared with the average capacity of these batteries (in the three initial cycles) before the very first measurement (after stabilizing the SEI layer). If the measured average capacity was less than 4% of its original capacity, the batteries were replaced with new ones.

The verification of Equations (4) and (6) for the studied batteries (Table 1) was performed in paper [10]. The experimental studies showed that when using Equations (4) and (6) in model (1), the relative error in the calculation of the battery's residual capacity was less than 4% [9]. Notably, when using Equation (3) in model (1), the relative error was about 5% [10].

Therefore, it follows from the experimental studies [10,12,13] that in practice, the capacity of the lithium-ion batteries almost does not change within the temperature range from 25 °C to 55 °C (the relative deviation of the capacity from the average value is less than 1%).

According to the procedure of experimental measurements (described above), at each discharge current, the released battery capacity was measured three times for three batteries of the same type. That is, nine measurements were performed at each discharge current. Then, the average value for these measurements was found, and it is this average value that is shown in all Figure 2. Using the averages in the Figure 2 has two advantages. First, the scatter of experimental values in the Figures is significantly reduced, which improves

its quality. Secondly, the error for the average value is $\sqrt{n}$ times less than the error for an individual measurement (n is the number of measurements at a certain discharge current).

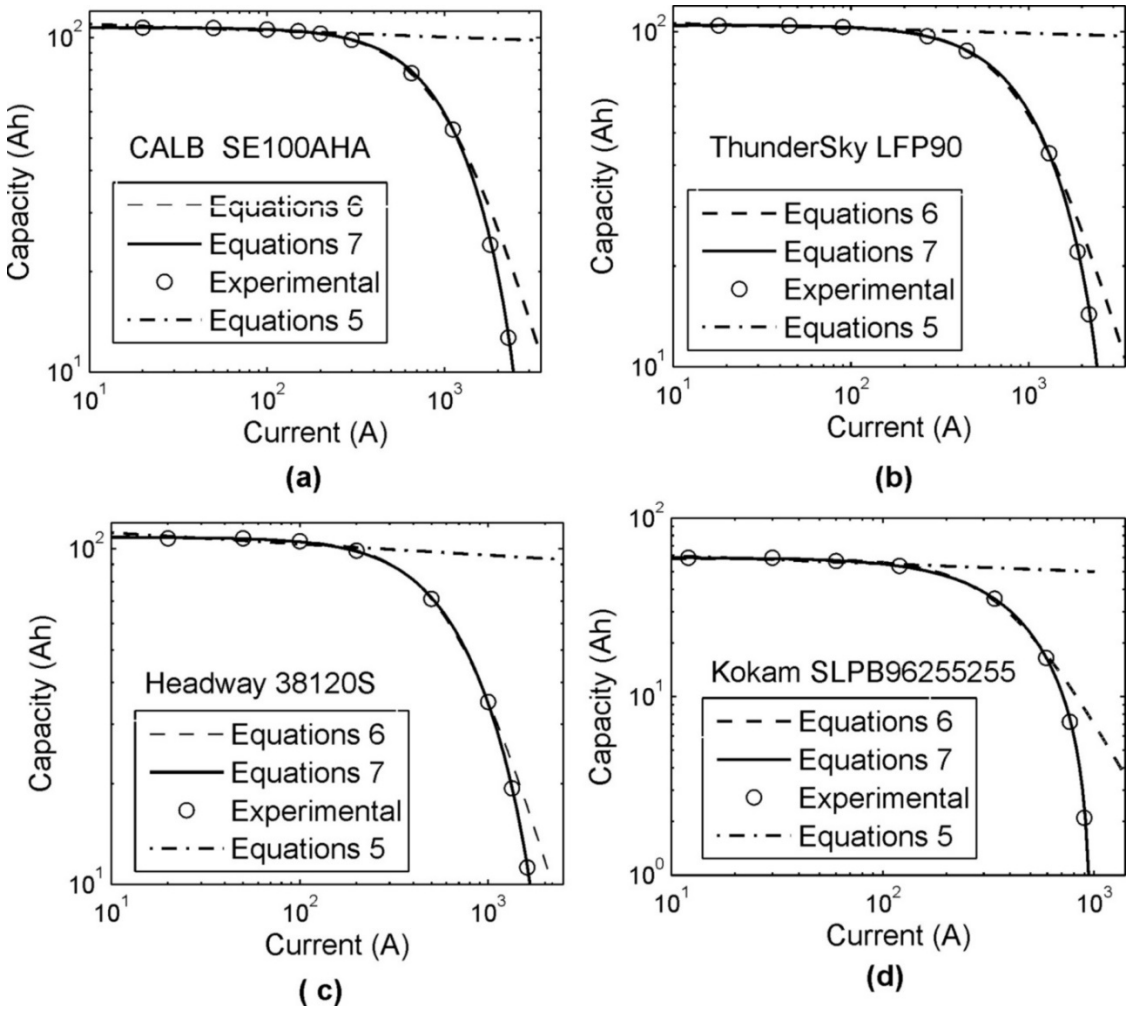

Figure 2. Comparison between Equations (5)–(7) and experimental data for automotive-grade lithium-ion batteries: (**a**) batteries CALB SE100AHA; (**b**) batteries ThunderSky LFP90; (**c**) batteries Headway 38120S; (**d**) batteries Kokam SLPB96255255.

The error of approximation of experimental data by Equations (5)–(7) determines the accuracy of the correspondence of these equations to the obtained experimental data.

The error in measuring the parameters of batteries of a certain type depends not only on the accuracy of the instruments, but also on various random processes in the manufacture of batteries and when they are discharged. Therefore, we found the true error of any measurement by statistical methods by measuring each experimental point several times.

In this article, the approximation error by Equations (5)–(7) of the experimental data and their optimal parameters were found using the least square method and the Levenberg–Marquardt optimization procedure in the framework of a statistical computer program.

It should be noted that when finding both the experimental data approximation errors by Equations (5)–(7) and the optimal parameters of these equations, all measured capacity values were used, not just the averages from Figure 2.

3. Results

Figure 2 show the experimental data for the batteries under study (see Table 1). Additionally, it makes a comparison between Equations (5)–(7) and the obtained experimental data.

In order to make the difference between Equations (6) and (7) clearer at the large discharge currents in Figure 2, all the values are presented in the logarithmic coordinate system.

After that, the experimental data obtained (Figure 2) approximation was performed using Equations (5)–(7), and the optimal parameters for these equations were found. The approximation was performed using the least square method and the optimization procedure by Levenberg–Marquardt. The values of the optimal parameters found are presented in Tables 2–4 for Equations (5)–(7), respectively.

Table 2. Optimal values of parameters for generalized Peukert's Equation (6).

Parameters	CALB $LiFePO_4$	ThunderSky $LiFePO_4$	$LiFePO_4$	Kokam $LiCoO_2$
n	1.87	1.87	1.98	2.14
C_m (Ah)	106.9	104.5	107.8	59.4
$i0$ (A)	1107.8	1088.2	692.9	391.9
δ (%) [1]	3.1	3.5	3.4	3.6

[1] Relative error of experimental data approximation by Equation (6) in Figure 2.

Table 3. Optimal values of parameters for modified Peukert's Equation (7).

Parameters	CALB $LiFePO_4$	ThunderSky $LiFePO_4$	Headway $LiFePO_4$	Kokam $LiCoO_2$
n	1.62	1.52	1.58	1.43
C_m (Ah)	107.1	104.9	108.6	60.4
$i0$ (A)	1431.8	1478.7	886.6	578.2
$i1$ (A)	3241.4	3138.6	2305.5	974.4
δ (%) [1]	1.1	1	0.9	1.2
R (mΩ)	0.259	0.258	0.568	1.406

[1] Relative error of experimental data approximation by Equation (7) in Figure 2.

Table 4. Optimal values of parameters for classical Peukert's Equation (5).

Parameters	CALB$LiFePO_4$	ThunderSky $LiFePO_4$	Headway $LiFePO_4$	Kokam $LiCoO_2$
n	0.019	0.015	0.033	0.044
A	114.5	109.8	120.6	68.074
i_{max} (A) [2]	200	185	200	118
δ (%) [1]	0.65	0.82	2.06	2.19

[1] Relative error of experimental data approximation by Equation (5) in Figure 2. [2] The maximum current at which the Peukert Equation (5) is applicable for the batteries under study.

For Equation (7), the optimal parameters (Table 3) were found using all the experimental values obtained. For Equation (6), the optimal parameters (Table 2) were found using experimental values at discharge currents from zero to the second inflection point of the experimental curve $C(i)$ (that is, up to about currents $i0$ (Table 2)).

Equation (5) is applicable only in the range of the discharge currents from zero to the first inflection point (Figure 1) of the experimental function $C(i)$ for the lithium-ion batteries [31]. That is why, as for the optimal parameters of Equation (5), they were found only with the use of the experimental values from this range of the discharge currents (Table 4).

In Table 4, i_{max} is the value of the current starting from which the error of approximation of the experimental data by Equation (5) begins to increase. Usually, this current is slightly larger than the current corresponding to the first inflection point of the experimental function $C(i)$. Thus, i_{max} is the top current, at which the Peukert Equation (5) is applicable for the batteries under study.

4. Discussion

Equation (7) approximates the experimental data at any discharge current. Notably, for the error of the experimental data approximation, when the approximation was made using Equation (7) (which does take into account the internal resistance of a battery), the error was almost thrice less than in the case of Equation (6) (which does not take into account the internal resistance of a battery) (Tables 2 and 3). Thus, this study proves that

the reason for the drop in the capacity released by the batteries at the very large discharge currents is due to the voltage drop in the internal resistance of the batteries.

Now, using the found ratios (8), we estimate the internal resistance of the studied batteries.

$$R = \frac{E - u_k - u_r}{i1} \tag{9}$$

The values of parameter $i1$ for the batteries under study are shown in Table 3, and the values of parameter u_k (lower cutoff) are shown in Table 1.

The values of parameters E and u_r were found in separate experiments as they depend very much on relaxation processes. To determine parameters E and u_r, at first, the batteries were stabilized by performing five initial cycles (Table 1). Then, five initial measuring cycles were performed with the battery's EMF measurement after each round of charging and four hours of relaxation. Using the obtained values, we calculated the EMF value to be average for the batteries and the absolute measurement error. As a result, the following values were obtained for the EMF of the charged batteries: $E = 3.55 \pm 0.02$ V (for the batteries $LiFePO_4$) and $E = 4.18 \pm 0.02$ V (for the battery $LiCoO_2$). After the EMF measurement, the batteries were discharged (in our initial measuring cycles), and the dependence of the battery's voltage on its released capacity, $U(C)$, was found. Using the experimental function $U(C)$, we found the voltage drop due to the relaxation processes in the discharge process beginning, i.e., u_r.

As a result, for parameter u_r, the following values were found: $u_r = 0.24 \pm 0.02$ V (for the batteries $LiFePO_4$) and $u_r = 0.11 \pm 0.02$ V (for the batteries $LiCoO_2$).

Based on the obtained values for all the parameters, the internal resistance for all the types of batteries under study was found from Equation (9). The results of calculating the internal resistance of the batteries under study are presented in Table 3.

The comparison between the obtained values of the internal resistances (Table 3) and the experimental data (Figure 2) lets us conclude the following: The greater the internal resistance of the battery (Kokam $LiCoO_2$), the lower discharge currents will be ($i0 = 578.2$ A), at which this resistance must be taken into account, i.e., at which Equation (7) must be used instead of Equation (6).

Additionally, a number should be noted regarding the advantages of using Equations (6) and (7) in various analytical models as compared to the classical Peukert Equation (5).

Firstly, in Equations (6) and (7), all the parameters (C_m, $i0$, $i1$, n) have a clear electrochemical meaning, while in Equation (5), the parameters (A, n) are just empirical constants. Indeed, the meaning of the parameters (C_m, $i0$, $i1$) is evident from Equations (6) and (7), while the parameter (n) from Equation (6) is equal to

$$n = -4 \lim_{i \to i0} \frac{d(C(i)/C_m)}{d(i/i0)} \tag{10}$$

Thus, the parameter (n) is equal to the rate of decrease in the released capacity by the batteries depending on the discharge current (at the point $i = i0$) in relative coordinates ($i/i0$, C/C_m). The parameter (n) has a similar meaning in Equation (7) too.

It should be noted that the values of the currents ($i0$, $i1$) depend not only on the battery capacity but also on the electrodes' material and the design features of the battery. This fact follows from the fact that the rations $i0/C_m$ = (14.318, 16.43, 8.866, 9.637) and $i1/C_m$ = (32.414, 34.873, 23.055, 16.24) for the batteries CALB, ThunderSky, Headway, and Kokam (Table 3) differ greatly; notably, this difference is great both in the case of batteries with the same cathodes ($LiFePO_4$) and in the case of batteries with different cathodes ($LiFePO_4$ and $LiCoO_2$).

Secondly, with very high discharge currents, there is a current value at which (already at the moment, when the battery is switched on for discharge) the voltage at the terminals of the battery will be equal to the lower cutoff of voltage. At this current $i1$, the battery capacity will be zero when the battery is turned on for discharge. Notwithstanding,

currently, this obvious fact is not taken into account by any of the existing equations, except for Equation (7).

Thus, for many lithium-ion batteries (in analytical models) at normal operating discharging currents, the classical Peukert Equation (5) [9] can be used. However, from a theoretical point of view, it is necessary to use Equation (7) as the more correct one. These things considered, for lithium-ion batteries with significant internal resistance, it is also necessary to use Equation (7).

5. Conclusions

The conducted experimental studies allow us to draw a number of conclusions.

Firstly, the classical Peukert Equation (5) is applicable for automotive-grade lithium-ion batteries within the range of discharge currents from $0.2C_n$ to $i_{\max}$ (approximately $2C_n$) (Table 4). Note also that current $i_{\max}$ is approximately equal to the current corresponding to the first inflection point of the experimental function $C(i)$ (Figures 1 and 2). At current values less than $0.2C_n$, the classical Peukert Equation (5) is not applicable for the batteries under study. When the discharge currents obtain less, the capacity tends to infinity, which does not fit the experimental data. It should be noted that the operating currents of the batteries under study during their operation in cars just belong to the range of the discharge currents from $0.2C_n$ to $2C_n$. This fact explains the successful use of the classical Peukert Equation (5) in the Hausmann model (1) for the determination of the battery's residual capacity.

Secondly, the generalized Peukert Equation (6) is applicable in the range of the discharge currents from zero to $i0$. Notably, current $i0$ corresponds approximately to the second inflection point of the experimental function $C(i)$ (Figures 1 and 2). Notwithstanding that during the operation of the studied batteries in cars, the operating currents are mainly within the range of the discharge currents from $0.2C_n$ to $2C_n$, yet, the generalized Peukert Equation (6) using in the Hausmann model (1) has a number of advantages. Firstly, during the operation of the batteries under study, their discharge is possible with currents less than $0.2C_n$. In this case, the classical Peukert Equation (5) is not applicable. That is why the use of Equation (5) at these currents in the Hausmann model (1) will lead to significant errors when determining the residual capacity of these batteries. Secondly, during the operation of the studied batteries in cars, the possibility is not excluded of the appearance of short-term currents exceeding the limit current $i_{\max}$ (around $2C_n$). In this case, the classical Peukert Equation (5) is not applicable. Hence, the use of Equation (5) in the Hausmann model (1) with very large short-term currents will also lead to significant errors. So, the conducted studies show clearly that the use of Equation (6) in the Hausmann model (1) is preferable as compared to the use of the classical Peukert Equation (5).

Thirdly, the modified Peukert Equation (7) is applicable at any discharge current. In addition, the error of the experimental data approximation using Equation (7) is more than twice less than in the case of Equation (6) (Tables 2 and 3). This is despite the fact that when approximating using Equation (7), significantly more experimental data is used (Table 3) than when approximating using Equation (6) (Figure 2). Thus, the accuracy of approximation by Equation (7) is not related to an increase in the number of factors in the equation but to the fact that Equation (7) more accurately reflects the processes in batteries. However, this can be seen in Figure 2.

It should also be noted that only Equation (7) indicates the existence of a limiting discharge current (which is experimentally observed in all batteries), at which, at the moment the battery is turned on for discharge, the released capacity will already be equal to zero.

These facts alone show the advantage of using Equation (7) in the Hausmann model (1) as compared to Equations (5) and (6).

The Peukert Equation (5) and its generalization (6) are used in many analytical models [9,10,33,34]. That is why problems such as the determination of the applicability of Equations (5)–(7) for automotive-grade lithium-ion batteries, their refinement, and the

identification of the physical meaning of the parameters used in those equations are of great theoretical and practical importance.

Author Contributions: Conceptualization, N.E.G.; methodology, N.N.Y.; software, M.S.L.; validation, N.N.Y.; formal analysis, M.S.L.; data curation, D.N.G.; visualization, N.N.Y.; supervision, D.N.G.; project administration, D.N.G. All authors have read and agreed to the published version of the manuscript.

Funding: This research received no external funding.

Institutional Review Board Statement: Not applicable.

Informed Consent Statement: Not applicable.

Data Availability Statement: Not applicable.

Conflicts of Interest: The authors declare no conflict of interest.

References

1. Blomgren, G.E. The Development and Future of Lithium Ion Batteries. *J. Electrochem. Soc.* **2017**, *164*, A5019–A5025. [CrossRef]
2. Zubi, G.; Dufo-López, R.; Carvalho, M.; Pasaoglu, G. The lithium-ion battery: State of the art and future perspectives. *Renew. Sustain. Energy Rev.* **2018**, *89*, 292–308. [CrossRef]
3. Kim, S.U.; Albertus, P.; Cook, D.; Monroe, C.W.; Christensen, J. Thermoelectrochemical simulations of performance and abuse in 50-Ah automotive cells. *J. Power Sources* **2014**, *268*, 625–633. [CrossRef]
4. Lipu, M.S.H.; Hannan, M.A.; Hussain, A.; Hoque, M.M.; Ker, P.J.; Saad, M.H.M.; Ayob, A. A review of state of health and remaining useful life estimation methods for lithium-ion battery in electric vehicles: Challenges and recommendations. *J. Clean. Prod.* **2018**, *205*, 115–133. [CrossRef]
5. Hannan, M.A.; Lipu, M.S.H.; Hussain, A.; Mohamed, A. A review of lithium-ion battery state of charge estimation and management system in electric vehicle applications: Challenges and recommendations. *Renew. Sustain. Energy Rev.* **2017**, *78*, 834–854. [CrossRef]
6. Fan, G.; Pan, K.; Canova, M.; Marcicki, J.; Yang, X.G. Modeling of Li-Ion cells for fast simulation of high C-rate and low temperature operations. *J. Electrochem. Soc.* **2016**, *163*, A666–A676. [CrossRef]
7. Arunachalam, H.; Onori, S.; Battiato, I. On Veracity of Macroscopic Lithium-Ion Battery Models. *J. Electrochem. Soc.* **2015**, *162*, A1940–A1951. [CrossRef]
8. Cugnet, M.; Laruelle, S.; Grugeon, S.; Sahut, B.; Sabatier, J.; Tarascon, J.-M.; Oustaloup, A. A mathematical model for the simulation of new and aged automotive lead-acid batteries. *J. Electrochem. Soc.* **2009**, *156*, A974–A985. [CrossRef]
9. Hausmann, A.; Depcik, C. Expanding the Peukert equation for battery capacity modeling through inclusion of a temperature dependency. *J. Power Sources* **2013**, *235*, 148–158. [CrossRef]
10. Galushkin, N.E.; Yazvinskaya, N.N.; Galushkin, D.N. Generalized analytical model for capacity evaluation of automotive-grade lithium batteries. *J. Electrochem. Soc.* **2015**, *162*, A308–A314. [CrossRef]
11. Tremblay, O.; Dessaint, L.A. Experimental validation of a battery dynamic model for EV applications. *World Electr. Veh. J.* **2009**, *3*, 289–298. [CrossRef]
12. Galushkin, N.E.; Yazvinskaya, N.N.; Galushkin, D.N. A Critical Review of Using the Peukert Equation and its Generalizations for Lithium-Ion Cells. *J. Electrochem. Soc.* **2020**, *167*, 120516. [CrossRef]
13. Galushkin, N.E.; Yazvinskaya, N.N.; Galushkin, D.N. Analysis of Generalized Peukert's Equations for Capacity Calculation of Lithium-Ion Cells. *J. Electrochem. Soc.* **2020**, *167*, 013535. [CrossRef]
14. Galushkin, N.E.; Yazvinskaya, N.N.; Galushkin, D.N.; Galushkina, I.A. Generalized analytical models of batteries' capacitance dependence on discharge currents. *Int. J. Electrochem. Sci.* **2014**, *9*, 4429–4439.
15. Galushkin, N.E.; Yazvinskaya, N.N.; Galushkin, D.N. Model of relaxation processes in batteries. *ECS Electrochem. Lett.* **2015**, *4*, A94–A96. [CrossRef]
16. Galushkin, N.E.; Yazvinskaya, N.N.; Galushkin, D.N. Analytical model of thermal runaway in alkaline batteries. *Int. J. Electrochem. Sci.* **2018**, *13*, 1275–1282. [CrossRef]
17. Galushkin, N.E.; Yazvinskaya, N.N.; Galushkin, D.N. Thermal runaway as a new high-performance method of desorption of hydrogen from hydrides. *Int. J. Hydrog. Energy* **2016**, *41*, 14813–14819. [CrossRef]
18. Galushkin, N.E.; Yazvinskaya, N.N.; Galushkin, D.N. Mechanism of thermal runaway as a cause of Fleischmann-Pons effect. *J. Electroanal. Chem.* **2020**, *870*, 114237. [CrossRef]
19. Galushkin, N.E.; Yazvinskaya, N.N.; Galushkin, D.N. Study of thermal runaway electrochemical reactions in alkaline batteries. *J. Electrochem. Soc.* **2015**, *162*, A2044–A2050. [CrossRef]
20. Galushkin, N.E.; Yazvinskaya, N.N.; Galushkin, D.N. Nickel-cadmium batteries with pocket electrodes as hydrogen energy storage units of high-capacity. *J. Energy Storage* **2021**, *39*, 102597. [CrossRef]

21. Galushkin, N.E.; Yazvinskaya, N.N.; Galushkin, D.N. Pocket electrodes as hydrogen storage units of high-capacity. *J. Electrochem. Soc.* **2017**, *164*, A2555–A2558. [CrossRef]
22. Geng, P.; Wang, L.; Du, M.; Bai, Y.; Li, W.; Liu, Y.; Chen, S.; Braunstein, P.; Xu, Q.; Pang, H. MIL-96-Al for Li–S Batteries: Shape or Size? *Adv. Mater.* **2021**, *34*, 2107836. [CrossRef]
23. Li, W.; Guo, X.; Geng, P.; Du, M.; Jing, Q.; Chen, X.; Zhang, G.; Li, H.; Xu, Q.; Braunstein, P.; et al. Rational Design and General Synthesis of Multimetallic Metal–Organic Framework Nano-Octahedra for Enhanced Li–S Battery. *Adv. Mater.* **2021**, *33*, 2105163. [CrossRef] [PubMed]
24. Coleman, M.; Lee, C.K.; Zhu, C.; Hurley, W.G. State-of-charge determination from EMF voltage estimation: Using impedance, terminal voltage, and current for lead-acid and lithium-ion batteries. *IEEE Trans. Ind. Electron.* **2007**, *54*, 2550–2557. [CrossRef]
25. Rakhmatov, D.; Vrudhula, S.; Wallach, D.A. A model for battery lifetime analysis for organizing applications on a pocket computer. *IEEE Trans. Very Large Scale Integr. Syst.* **2003**, *11*, 1019–1030. [CrossRef]
26. He, W.; Williard, N.; Chen, C.; Pecht, M. State of charge estimation for electric vehicles batteries using unscented Kalman filtering. *Microelectron. Reliab.* **2013**, *53*, 840–847. [CrossRef]
27. Han, J.; Kim, D.; Sunwoo, M. State-of-charge estimation of lead-acid batteries using an adaptive extended Kalman filter. *J. Power Sources* **2009**, *188*, 606–612. [CrossRef]
28. He, H.; Zhang, X.; Xiong, R.; Xu, Y.; Guo, H. Online model-based estimation of state-of-charge and open-circuit voltage of lithium-ion batteries in electric vehicles. *Energy* **2012**, *39*, 310–318. [CrossRef]
29. He, Y.; Liu, X.T.; Zhang, C.B.; Chen, Z.H. A new model for State-of-Charge (SOC) estimation for high-power Li-ion batteries. *Appl. Energy* **2013**, *101*, 808–814. [CrossRef]
30. Buchmann, I. *Batteries in a Portable World*; Cadex Electronics Inc.: Richmond, BC, Canada, 2016.
31. Galushkin, N.E.; Yazvinskaya, N.N.; Ruslyakov, D.V.; Galushkin, D.N. Analysis of Peukert and Liebenow Equations Use for Evaluation of Capacity Released by Lithium-Ion Batteries. *Processes* **2021**, *9*, 1753. [CrossRef]
32. Peukert, W. About the dependence of the capacity of the discharge current magnitude and lead acid batterie. *Elektrotech. Z.* **1897**, *20*, 287–288.
33. Nebl, C.; Steger, F.; Schweiger, H.-G. Discharge Capacity of Energy Storages as a Function of the Discharge Current—Expanding Peukert's equation. *Int. J. Electrochem. Sci.* **2017**, *12*, 4940–4957. [CrossRef]
34. Wu, G.; Lu, R.; Zhu, C.; Chan, C.C. Apply a Piece-wise Peukert's Equation with Temperature Correction Factor to NiMH Battery State of Charge Estimation. *J. Asian Elect. Veh.* **2010**, *8*, 1419–1423. [CrossRef]
35. Shepherd, C.M. Design of Primary and Secondary Cells: II. An Equation Describing Battery Discharge. *J. Electrochem. Soc.* **1965**, *112*, 657. [CrossRef]